First in-situ observations of strong ionospheric perturbations generated by a powerful VLF ground-based transmitter

Michel Parrot, J.-A. Sauvaud, Jean-Jacques Berthelier, J.-P. Lebreton

First in-situ observations of strong ionospheric perturbations generated by a powerful VLF ground-based transmitter

M. Parrot,[1] J. A. Sauvaud,[2] J. J. Berthelier,[3] and J. P. Lebreton[4]

Received 16 January 2007; revised 23 April 2007; accepted 7 May 2007; published 12 June 2007.

[1] This paper is related to observations by the satellite DEMETER of strong ionospheric perturbations close to the VLF transmitter NWC in Australia (L = 1.41). Electrostatic waves from HF to ELF ranges are generated and strong turbulence appears. Fluctuations of electron and ion densities are observed as well as increase of temperature. The perturbations are located to the geographic North of the transmitter and cover an area of ~500,000 km^2 which is centred at the altitude of the satellite (700 km) around the magnetic field line at L = 1.41. The phenomenon is due to the electron and ion heating induced by the powerful transmitter VLF wave. This perturbation is in addition to the already known precipitation of energetic particles which interact with the VLF wave through a cyclotron resonance mechanism. The particle precipitation zone is located south of the transmitter at a slightly larger L-shell value (1.9).
Citation: Parrot, M., J. A. Sauvaud, J. J. Berthelier, and J. P. Lebreton (2007), First in-situ observations of strong ionospheric perturbations generated by a powerful VLF ground-based transmitter, *Geophys. Res. Lett.*, *34*, L11111, doi:10.1029/2007GL029368.

1. Introduction

[2] The ionospheric perturbations induced by the VLF transmitters have been studied for a long time. In the past the theoretical problems of non linear interaction between energetic electrons and coherent VLF waves were considered by many authors [e.g., *Helliwell*, 1967; *Nunn*, 1971, 1974, 1990; *Dowden et al.*, 1978; *Shklyar et al.*, 1992]. Theories concerning the generation mechanism of these triggered emissions have been reviewed by *Omura et al.* [1991]. Another review by *Parrot and Zaslavski* [1996] addressed the physical processes related to anthropogenic disturbances of the ionosphere including the effects of the VLF transmitters. Observations of electron precipitation by VLF transmitters have been made by *Koons et al.* [1981], *Inan et al.* [1982, 1985], *Imhof et al.* [1986], *Vampola* [1987, 1990], and more recently by *Sauvaud et al.* [2006]. *Inan et al.* [1984] presented maps of global electron precipitation zones induced by the major VLF transmitters (except NWC). But new insights have been recently developed which include NWC (U. S. Inan, personal communication, 2007). The involved mechanism is the well-known cyclotron resonance. The wave and the particles interact when the Doppler-shifted wave frequency seen by the particle is close to the electron gyrofrequency. The possible production of lower hybrid parametric instabilities by VLF transmitters has been studied by *Riggin and Kelley* [1982]. Another mechanism has been presented by *Bell and Ngo* [1988, 1990] and *Bell et al.* [1991] which attributes the excited lower hybrid waves to the electromagnetic whistler mode waves scattered from magnetic field aligned plasma density irregularities in the ionosphere. Concerning the plasma perturbations, heating by the VLF waves has been theoretically considered and it has been shown that the mechanism is efficient in the D region [*Galejs*, 1972; *Inan*, 1990; *Inan et al.*, 1992; *Barr and Stubbe*, 1992; *Rodriguez et al.*, 1994]. But no direct observations of plasma perturbations have been reported so far in the literature.

[3] This paper presents an analysis of the ionospheric perturbations observed by the DEMETER satellite in vicinity of the VLF transmitter NWC in Australia (21°47′S, 114°09′E) which is operating at 19.8 kHz. NWC is one of the most powerful VLF transmitters in the world (1000 kW) and it is located at a low L-shell value (L = 1.4). DEMETER was launched on June 29, 2004 on low-altitude polar orbit to study ionospheric perturbations in relation with the seismic activity and the anthropogenic activity [*Cussac et al.*, 2006]. The DEMETER payload will be briefly described in section 2. The data will be shown in section 3. Discussion and conclusions will be provided in section 4.

2. Wave and Plasma Experiments Onboard DEMETER

[4] The scientific payload of the DEMETER microsatellite is composed of several instruments which provide a nearly continuous survey of the plasma, waves and energetic particles around the Earth at an altitude of 700 km. The electric field experiment uses four electric probes to measure the three components of the electric field in a frequency range from DC up to 3.5 MHz. The search-coil magnetometer measures the three components of the magnetic field in a frequency range from a few Hz up to 20 kHz. The Langmuir probe gives access to the electron density and temperature. The thermal ion spectrometer measures the ion density, composition, temperature and flow velocity. A solid state energetic particle detector measures high energy electrons and protons looking in a direction perpendicular to the orbit plane, i.e. measuring particles with a mirror point in the vicinity of the satellite.

[1]Laboratoire de Physique et de Chimie de l'Environnement, Centre National de la Recherche Scientifique, Orléans, France.
[2]Centre d'Etude Spatiale des Rayonnements, Centre National de la Recherche Scientifique, Toulouse, France.
[3]Centre d'Etude des Environnements Terrestre et Planétaires, Saint Maur des Fossés, France.
[4]Research and Scientific Support Department, European Space Research and Technology Centre, European Space Agency, Noordwijk, Netherlands.

0094-8276/07/2007GL029368

Details about these experiments can be found in work by *Berthelier et al.* [2006a, 2006b], *Lebreton et al.* [2006], *Parrot et al.* [2006], and *Sauvaud et al.* [2006]. DEMETER is operated in two scientific modes: - A survey mode, where spectra of one electric and one magnetic component are computed onboard up to 20 kHz. with a frequency resolution of 19.25 Hz, - A burst mode where waveforms of one electric and one magnetic components are recorded up to 20 kHz, and waveforms of the six electromagnetic field components are recorded up to 1.25 kHz. DEMETER was launched on a polar and circular sun-synchronous orbit with an altitude of 710 km. Due to technical reasons data are only recorded at invariant latitudes less than $\sim 65°$. All data files and plots are organised by half-orbits [*Lagoutte et al.*, 2006]. The up-going half-orbits (invariant latitude between 65°S and 65°N) correspond to night time (22.30 LT) and the down-going half-orbits (invariant latitude between 65°N and 65°S) to day time (10.30 LT).

3. Data

3.1. Example of Perturbations Observed Close to NWC

[5] An example of the observed ionospheric perturbations is shown in Figure 1. It is related to data recorded on September 22, 2006 during night time. The plots which contain ionospheric parameters as a function of the time will be described from the top to the bottom. The top plot represents the onboard-computed spectrogram of an electric component in the HF range and the main feature is observed around 14.52.30 UT. It corresponds to an excitation close to the upper hybrid resonance in a frequency band between 1.6 and 1.9 MHz. At the time of observation, the electron gyrofrequency is equal to $\sim$ 1.03 MHz (the Earth's magnetic field is given by a model), and the plasma frequency is equal to $\sim$ 1.27 MHz (see the plot below). Then the value of the upper hybrid frequency is of the order of 1.63 MHz. The second plot is devoted to the onboard computed spectrogram of the same electric component in the VLF range up to 20 kHz. In the top of this plot horizontal lines show transmitter frequencies and the more intense one at 19.8 kHz is the NWC frequency. The vertical lines in the spectrogram are related to spherics. Around 14.52.30 UT it can be seen that the perturbation covers the whole frequency range. Electrostatic turbulence is observed at low frequencies and a very large broadening of the transmitter frequency can be noticed. In the perturbation area, the intensity of waves (mainly spherics) is also enhanced. The most important electrostatic noise between $\sim$10 and 20 kHz has a low frequency cut-off at the lower hybrid frequency which is over plotted with a white line on this VLF plot. The lower hybrid frequency is obtained using the electron density and the ion composition measured in-situ [*Berthelier et al.*, 2006b]. The variation of this lower hybrid frequency is due to the variation of the electron density (shown below) and the change of the effective ion mass (not shown). The next two plots represent respectively the electron density and the electron temperature measured by the Langmuir probe. Large fluctuations of these two parameters are observed in the same area. Finally the bottom plot shows the dramatic increase of the ion temperature measured by the ion spectrometer. At maximum it is nearly twice the background level. The geographic latitude and longitude, and the L value are shown below the plots.

3.2. Perturbation Zone

[6] The occurrence of these perturbations has been searched in the two-year DEMETER data base and 49 typical events with large ionospheric perturbations have been found between March 2005 and November 2006. These events have been visually selected using the VLF electric spectrogram of the quick-looks [*Lagoutte et al.*, 2006]. The geographical locations of these 49 night time perturbations have been reported in the map of Figure 2. The lines represent the projections of the orbits of the satellite on the surface of the Earth. Many of them are superposed due to the orbitography of the satellite. The star indicates the position of the transmitter NWC on the North-West coast of Australia. The perturbation area is observed at the North of the transmitter location and it covers an area of the order of 500,000 km^2. In fact the perturbations are locally observed in an area which is centred around the crossing (the square in Figure 2) between the orbit of the satellite at the altitude of 700 km and the magnetic field line (L = 1.41) whose South foot is at the transmitter location. On the other side, in the North hemisphere similar perturbations are also observed at nearly the same L value but with a much weaker intensity and only wave perturbations are detected.

4. Discussion and Conclusions

[7] In order to check if there is a parametric excitation of the lower hybrid waves by the coherent waves from NWC [*Riggin and Kelley*, 1982] a bicoherence analysis has been performed [see *Lagoutte et al.*, 1989, and references therein]. The event not shown here was selected when the satellite was in burst mode (to have waveforms) among the 49 cases where strong perturbations are observed. The VLF data up to 20 kHz were used. But the bicoherence spectrogram does not show any relation between the frequencies of the VLF spectrogram. In fact during this event the lower hybrid frequency ($\sim$18.8 kHz) is very close to the transmitter frequency (19.8 kHz) and the theory presented by *Bell and Ngo* [1988, 1990] is the most probable to explain the electrostatic wave enhancement. Electrostatic waves are excited by linear mode coupling when the electromagnetic VLF transmitter waves scatter from plasma density irregularities.

[8] The plasma perturbations are due to the electron and ion heating. It has been shown by *Rodriguez et al.* [1994] that the NAA transmitter (same power as NWC) can increase the night-time D region electron temperature by a factor of 3. The NWC transmitter is continuously operating and heating the D region above and, then, the perturbation is able to spread in the upper ionospheric levels where it can be observed by the satellite. It must be noticed that the heating is not continuous in the whole perturbation area and that striations appear. In the past density striations have been observed during HF heating experiments [*Fejer*, 1979; *Stubbe et al.*, 1982]. A strong enhancement of the electron temperature inside the striations was predicted by *Gurevich et al.* [1995], and *Vas'kov et al.* [1986] have shown that radiowave can excite the upper hybrid frequency. It is important to notice that the ionospheric perturbations

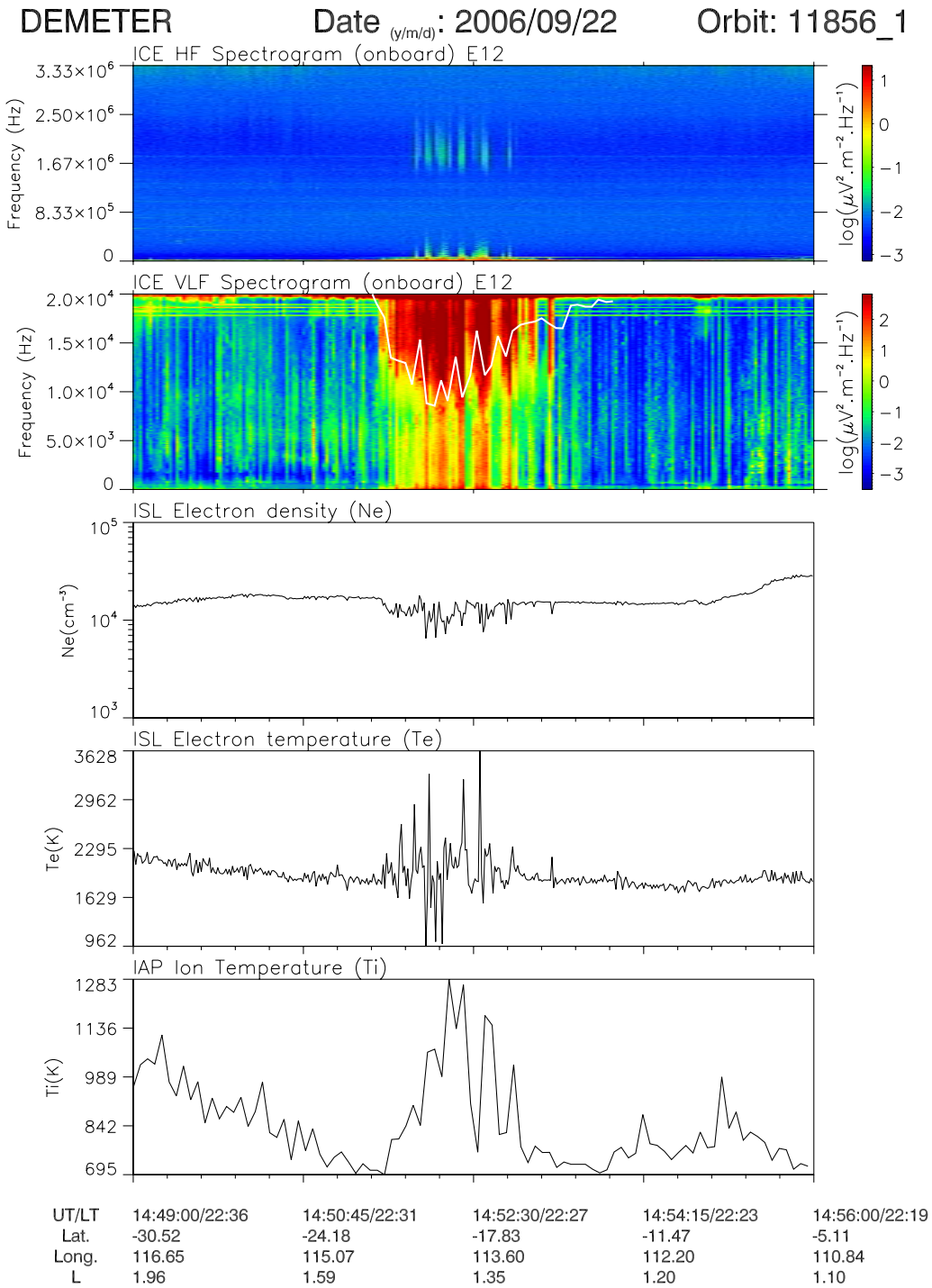

Figure 1. Data recorded on September 22, 2006 between 14.49.00 and 14.56.00 UT. From the top to the bottom the plots represent, the HF spectrogram of one electric component up to 3.33 MHz, the VLF spectrogram of the same component up to 20 kHz (the white line represents the lower hybrid frequency), the electron density, the electron temperature, and the ion temperature as function of the time. A large perturbation is observed at the North of the NWC location (21°47′S, 114°09′E).

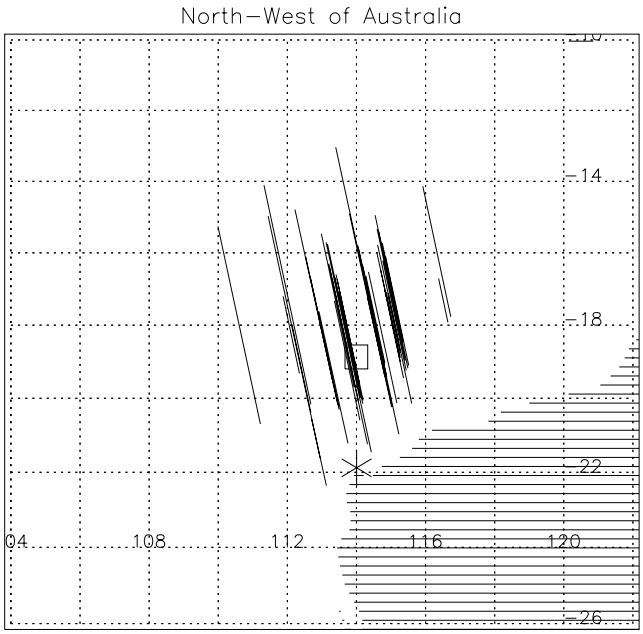

Figure 2. Map of the North-West coast of Australia. The straight lines are the projections of the parts of the DEMETER orbits where ionospheric perturbations similar to those shown in Figure 1 are observed. The square shows the geographical position of the crossing between the orbit of the satellite and the field line whose foot is at the NWC transmitter. The NWC position is indicated by a star.

reported here have also been observed at much higher latitudes by rocket [*LaBelle et al.*, 1986] and satellite [*Eriksson et al.*, 1994] associated with natural auroral activity. According to *Seyler* [1994], wave phenomena near the lower hybrid frequency are associated with plasma density depletions and a ponderomotive force can lead to the formation of this density cavity in which lower hybrid wave energy is concentrated. This ponderomotive force could be either NWC waves as it is shown here or natural whistler waves. The fact that man-made waves can reproduce at low latitudes natural effects observed in the auroral zone opens new perspectives for theoretical modelling.

[9] Concerning the precipitated electrons induced by the coherent VLF wave of NWC, DEMETER does not detect electrons at the same location where the strong ionospheric perturbations are observed but at a higher L value. Figure 3 represents an extended view of the data shown in Figure 1. The plot now corresponds to the complete half orbit from the South hemisphere to the North hemisphere. The top plot shows the VLF spectrogram of the electric component from 15 to 20 kHz. The perturbation due to the transmitter starting at 14.51.37 UT is evidently seen. The bottom plot displays the energetic electron flux integrated in three different energy bands [*Sauvaud et al.*, 2006], the black line being devoted to the lowest energy band (90.7–526.8 keV). This plot clearly shows the energetic particles in the outer radiation belt at high L values in both hemispheres. In the south hemisphere it ends around 14.47.20 UT (L = 2.5) and then it is the slot region. Two other increases in the inner belt location are also detected at 14.49.00 UT and

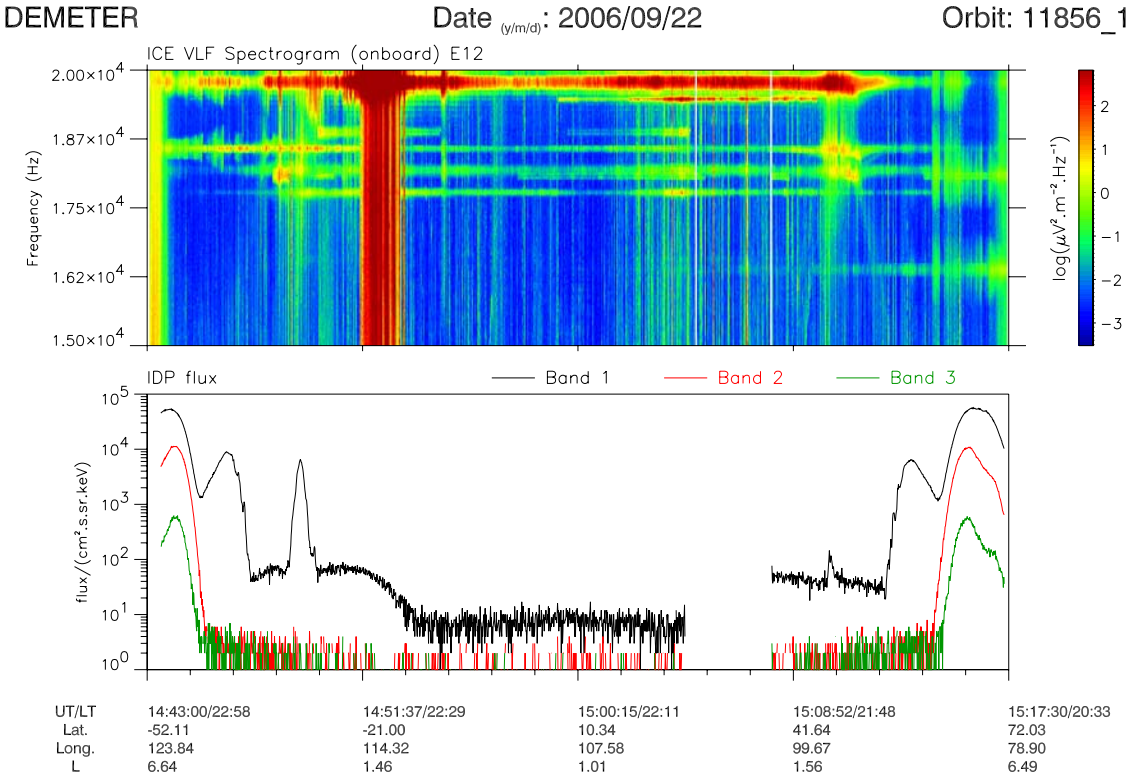

Figure 3. Extended plot of the data shown in Figure 1 along a complete half-orbit. (top) VLF spectrogram of an electric component from 15 to 20 kHz. (bottom) Integrated flux of the energetic particles in three bands (black line from 90.7 keV to 526.8 keV, red line from 526.8 keV to 971.8 keV, and green line from 971.8 keV to 2342.4 keV). The gap in the data is due to the fact that the information is not present during the burst mode. Orbital parameters are shown below the plots.

15.10.20 UT, the largest one being in the south hemisphere. These two increases of the particle flux are at the same L value (1.85). Nothing is observed at the location of the strong perturbation (L = 1.41). These increases of the energetic electron flux are practically always observed at the same L values (1.8–1.9) when the satellite is at the longitude of the transmitter. This is in agreement with the theoretical map of particle precipitation induced by NWC (U. S. Inan, personal communication, 2007). At L = 1.8 the cyclotron harmonic equatorial resonant energy for a wave frequency equal to ~20 kHz is ~100 keV [*Imhof et al.*, 1986; *Abel and Thorne*, 1998] and it corresponds to the energy range (90.7–526.8 keV) observed by DEMETER in relation with NWC. It has been shown by *Inan et al.* [1984] that the maximum precipitation region does not always coincide with the location of the transmitter because it depends on the geographic position of the transmitter, its power and its operating frequency. For transmitters at low L values it generally appears at higher L values because the distance from the source is balanced by the increase in particle flux with L. The electrons have typical decreasing energy with increasing L. It can be also seen in the top plot of Figure 3 that the transmitter signals are broadened close to 15.10.20 UT where the particles are precipitated because it increases ionospheric turbulence [*Bell and Ngo*, 1988, 1990].

[10] Only precipitations of particles by VLF transmitters and indirect manifestation of heating [*Inan*, 1990] have been reported in the past. Other perturbations in the upper ionosphere were expected [*Bell and Ngo*, 1988, 1990]. With the low orbiting satellite DEMETER which can measure wave and plasma parameters all around the Earth with a good resolution, it was possible to show for the first time the complete in-situ perturbations of the ionospheric plasma in night time. Nothing is observed during day time in the zone shown in Figure 2. Observations are only during night time because the ionospheric D region disappears and the wave absorption is reduced below the interaction area where the heating occurs. In day time the electron density gradients are strong and the absorption zone is narrow. Perturbations are also observed with other powerful transmitters such as NAA in US (44°39N, 67°17W). But it is located at a more high L value (2.9) and the natural electromagnetic noise which exists close to the sub-auroral zone prevents us from well detecting the VLF wave transmitter effect on the plasma parameters.

[11] **Acknowledgments.** The authors thank CNES people involved in the mission development of the DEMETER satellite and those currently in charge of the operations in Toulouse. They are grateful for the support of the DEMETER mission centre engineers (J.-Y. Brochot and D. Lagoutte) in Orléans. They thank U. S. Inan for useful discussions.

References

Abel, B., and R. M. Thorne (1998), Electron scattering loss in Earth's inner magnetosphere: 1. Dominant physical processes, *J. Geophys. Res.*, *103*, 2385–2396.

Barr, R., and P. Stubbe (1992), VLF heating of the lower ionosphere: Variation with magnetic latitude and electron density profile, *Geophys. Res. Lett.*, *19*, 1747–1750.

Bell, T. F., and H. D. Ngo (1988), Electrostatic waves stimulated by coherent VLF signals propagating in and near the inner radiation belt, *J. Geophys. Res.*, *93*, 2599–2618.

Bell, T. F., and H. D. Ngo (1990), Electrostatic lower hybrid waves excited by electromagnetic whistler mode waves scattering from planar magnetic-field-aligned plasma density irregularities, *J. Geophys. Res.*, *95*, 149–172.

Bell, T. F., R. A. Helliwell, and M. K. Hudson (1991), Lower hybrid waves excited through linear-mode coupling and the heating of ions in the auroral and subauroral magnetosphere, *J. Geophys. Res.*, *96*, 11,379–11,388.

Berthelier, J. J., et al. (2006a), ICE, The electric field experiment on DEMETER, *Planet. Space Sci.*, *54*, 456–471.

Berthelier, J. J., et al. (2006b), IAP, the thermal plasma analyzer on DEMETER, *Planet. Space Sci.*, *54*, 487–501.

Cussac, T., et al. (2006), The DEMETER microsatellite and ground segment, *Planet. Space Sci.*, *54*, 413–427, doi:10.1016/j.pss.2005.10.013.

Dowden, R. L., A. D. McKay, L. E. S. Amon, H. C. Koons, and M. H. Dazy (1978), Linear and nonlinear amplification in the magnetosphere during a 6.6-kHz transmission, *J. Geophys. Res.*, *83*, 169–181.

Eriksson, A. I., B. Holback, P. O. Dovner, R. Boström, G. Holmgren, M. André, L. Eliasson, and P. M. Kintner (1994), Freja observations of correlated small-scale density depletions and enhanced lower hybrid waves, *Geophys. Res. Lett.*, *21*, 1843–1846.

Fejer, J. A. (1979), Ionospheric modification and parametric instabilities, *Rev. Geophys.*, *17*, 135–153.

Galejs, J. (1972), Ionospheric interaction of VLF radio waves, *J. Atmos. Terr. Phys.*, *34*, 421–436.

Gurevich, A. V., K. P. Zybin, and A. V. Lukyanov (1995), Stationary striation developed in the ionospheric modification, *Phys. Rev. Lett.*, *75*(13), 2622–2625.

Helliwell, R. A. (1967), A theory of discrete VLF emissions from the magnetosphere, *J. Geophys. Res.*, *72*, 4773–4790.

Inan, U. S. (1990), VLF heating of the lower ionosphere, *Geophys. Res. Lett.*, *17*, 729–732.

Inan, U. S., T. F. Bell, and H. C. Chang (1982), Particle precipitation induced by short-duration VLF waves in the magnetosphere, *J. Geophys. Res.*, *87*, 6243–6264.

Inan, U. S., H. C. Chang, and R. A. Helliwell (1984), Electron precipitation zones around major ground-based VLF signal sources, *J. Geophys. Res.*, *89*, 2891–2906.

Inan, U. S., H. C. Chang, R. A. Helliwell, W. L. Imhof, J. B. Reagan, and M. Walt (1985), Precipitation of radiation belt electrons by man-made waves: A comparison between theory and measurement, *J. Geophys. Res.*, *90*, 359–369.

Inan, U. S., J. V. Rodriguez, S. Lev-Tov, and J. Oh (1992), Ionospheric modification with a VLF transmitter, *Geophys. Res. Lett.*, *19*, 2071–2074.

Imhof, W. L., H. D. Voss, M. Walt, E. E. Gaines, J. Mobilia, D. W. Datlowe, and J. B. Reagan (1986), Slot region electron precipitation by lightning, VLF chorus, and plasmaspheric hiss, *J. Geophys. Res.*, *91*, 8883–8894.

Koons, H. C., B. C. Edgar, and A. L. Vampola (1981), Precipitation of inner zone electrons by whistler mode waves from the VLF transmitters UMS and NWC, *J. Geophys. Res.*, *86*, 640–648.

LaBelle, J., P. M. Kintner, A. W. Yau, and B. A. Whalen (1986), Large amplitude wave packets observed in the ionosphere in association with transverse ion acceleration, *J. Geophys. Res.*, *91*, 7113–7118.

Lagoutte, D., F. Lefeuvre, and J. Hanasz (1989), Application of bicoherence analysis in study of wave interactions in space plasma, *J. Geophys. Res.*, *94*, 435–442.

Lagoutte, D., et al. (2006), The DEMETER science mission centre, *Planet. Space Sci.*, *54*, 428–440.

Lebreton, J. P., et al. (2006), The ISL Langmuir probe experiment and its data processing onboard DEMETER: Scientific objectives, description and first results, *Planet. Space Sci.*, *54*, 472–486.

Nunn, D. (1971), A theory of VLF emissions, *Planet. Space Sci.*, *19*, 1141–1167.

Nunn, D. (1974), A self-consistent theory of triggered VLF emissions, *Planet. Space Sci.*, *22*, 349–378.

Nunn, D. (1990), The numerical simulation of VLF nonlinear wave-particle interactions in collision-free plasmas using the Vlasov hybrid simulation technique, *Comput. Phys. Commun.*, *60*, 1–25.

Omura, Y., D. Nunn, H. Matsumoto, and M. J. Rycroft (1991), A review of observational, theoretical, and numerical studies of VLF triggered emissions, *J. Atmos. Terr. Phys.*, *53*, 351–368.

Parrot, M., and Y. Zaslavski (1996), Physical mechanisms of man-made influences on the magnetosphere, *Surv. Geophys.*, *17*, 67–100.

Parrot, M., et al. (2006), The magnetic field experiment IMSC and its data processing onboard DEMETER: Scientific objectives, description and first results, *Planet. Space Sci.*, *54*, 441–455.

Riggin, D., and M. C. Kelley (1982), The possible production of lower hybrid parametric instabilities by VLF ground transmitters and by natural emissions, *J. Geophys. Res.*, *87*, 2545–2548.

Rodriguez, J. V., U. S. Inan, and T. F. Bell (1994), Heating of the nighttime *D* region by very low frequency transmitters, *J. Geophys. Res.*, *99*, 23,329–23,338.

Sauvaud, J. A., et al. (2006), High energy electron detection onboard DEMETER: The IDP spectrometer, description and first results on the inner belt, *Planet. Space Sci.*, *54*, 502–511.

Seyler, C. E. (1994), Lower hybrid wave phenomena associated with density depletions, *J. Geophys. Res.*, *99*, 19,513–19,525.

Shklyar, D. R., D. Nunn, A. J. Smith, and S. S. Sazhin (1992), An investigation into the nonlinear frequency shift in magnetospherically propagated VLF pulses, *J. Geophys. Res.*, *97*, 19,389–19,402.

Stubbe, P., et al. (1982), Ionospheric modification experiments in northern Scandinavia, *J. Atmos. Terr. Phys.*, *44*, 1025–1029.

Vampola, A. L. (1987), Electron precipitation in the vicinity of a VLF transmitter, *J. Geophys. Res.*, *92*, 4525–4532.

Vampola, A. L. (1990), In-situ observations of magnetospheric electron scattering by a VLF transmitter, *J. Atmos. Terr. Phys.*, *52*, 377–384.

Vas'kov, V. V., et al. (1986), Excitation of upper hybrid resonance in the ionospheric plasma by an intense radio wave, *Sov. Phys. JETP Lett.*, Engl. Transl., *43*, 663–666.

J. J. Berthelier, CETP, Observatoire de Saint Maur, 4 Avenue de Neptune, F-94107 Saint Maur des Fossés cedex, France.

J. P. Lebreton, Research and Scientific Support Department, ESTEC, ESA, Noordwijk NL-2200 AG, Netherlands.

M. Parrot, LPCE, CNRS, 3A Avenue de la Recherche Scientifique, F-45071 Orléans cedex 2, France. (mparrot@cnrs-orleans.fr)

J. A. Sauvaud, CESR, CNRS, 9 avenue du Colonel Roche, F-31028 Toulouse cedex 4, France.